

Scope of the Copper Halide/Bipyridyl System Associated with Calixarene-Based Multihalides for the Synthesis of Well-Defined Polystyrene and Poly(meth)acrylate Stars

Stéphanie Angot, K. Shanmugananda Murthy, Daniel Taton, and Yves Gnanou*

Laboratoire de Chimie des Polymères Organiques, ENSCPB-CNRS-Université Bordeaux 1, Avenue Pey Berland, BP 108, 33402 Talence Cedex, France

Received March 30, 2000; Revised Manuscript Received July 13, 2000

ABSTRACT: Novel multihalide compounds which were readily obtained by derivatization of 4-*tert*-butylcalix[4,6,8]arenes were used to initiate the atom transfer radical polymerization (ATRP) of styrene, *tert*-butyl acrylate (*t*-BuA), and methyl methacrylate (MMA), in the presence of CuX (X = Br or Cl) and 2,2'-bipyridyl. Well-defined polystyrene (PS) stars constituted of precisely four, six, and eight arms could be synthesized with a narrow polydispersity in this way. For instance, octafunctional polystyrene stars exhibiting molar masses as high as 600 000 g mol⁻¹ could be prepared. However, the polymerization had to be restricted to low conversion, typically below 15–20% to prevent stars from mutually coupling and avoid their contamination with species of higher functionality. Besides the concentration of polymeric radicals [P*], the factor that was found to play a significant role in the occurrence of star–star coupling is their overlapping concentration (C*): intermolecular coupling indeed appeared to be enhanced whenever stars crossed their C*, but ways to alleviate this phenomenon of star–star coupling were also reported. In the case of hexa- and tetrafunctional PS stars, well-defined samples could be obtained within a large range of conversion because of the lower probability of such hexa- and tetraarmed species to get coupled. With octaarmed poly(methyl methacrylate) stars as well, the polymerization had to be discontinued at relatively low conversion in order to isolate samples with the expected functionality of 8, although this class of polymeric radicals tend to disproportionate rather than to recombine upon reaction. In contrast, no such side reactions could be detected while synthesizing poly(*tert*-butyl acrylate) stars, because the ATRP of *t*-BuA is associated with a much lower equilibrium constant (K_{eq}) between dormant and active species—and therefore to a lower concentration of growing radicals for a same initial concentration of initiator—than in the case of styrene or MMA. The functionality of the stars obtained was checked by comparing their molar mass with that of their individual arms isolated after hydrolysis of the ester functions of the central core. The viscometric characterization also attested to the well-defined character of the star polymers generated from the calixarene derivatized initiators, as confirmed by the comparison of their intrinsic viscosity with that of linear homologues of same molar mass.

Introduction

Among all branched architectures, star polymers correspond to the simplest possible assembling of macromolecular chains in a branched structure since they involve only one central branching point per macromolecule. Star polymers with a precise number of arms have been quite useful in providing acute insight into how branching affects the overall properties of polymers in solution or in the melt.¹ The synthesis of well-defined star polymers that consist of a precise number of arms of same size calls for the use of the so-called “living/controlled” polymerization techniques.²

They are essentially two strategies to generate star-shaped polymers: one can either link a given number of linear chains to a same central core fitted with reactive functions (“arm-first” method)³ or grow branches from a multifunctional core that is able to initiate the polymerization in multiple directions (“core-first” method).⁴ Many star polymers exhibiting a precise number of arms were obtained following the former method. For instance, polystyrene stars constituted of 124 arms were produced by deactivation of “living” carbanionic linear polymers chains onto a dendritic molecule containing 124 chlorosilane functions.^{3h} Although straightforward,

this methodology could not be generalized to other stars than those based on polystyrene or polydienes because chlorosilane functions were found to satisfactorily react only with the corresponding carbanions. In the case of “living” carbocationic species, this strategy was shown successful with poly(vinyl ether)s only, the latter being quantitatively deactivated by multifunctional silyl ketene acetals to make the corresponding stars.⁵

In addition to these limitations related to the lack of appropriate multifunctional deactivating agents, the “arm-first” method generally entails an ultimate step of purification—aimed at avoiding the presence of linear chains added in excess—to drive the coupling reaction toward completion. Moreover, the stars obtained by the arm-first method do not carry a reactive function at their arm ends, unless specific initiators are used; such arm-first stars cannot therefore participate in further reactions.

The “core-first” method seems a priori more attractive, particularly with respect to the functionalization of the star arm ends. However, this technique also involves a major difficulty which is the design of multifunctional initiators from which branches can be grown. For instance, only two examples of a tricarbocationic initiator can be found in the recent literature.^{6a,b} Multifunctional anionic initiators based on alkoxides and that were used to prepare PEO stars with a precise number of arms are, however, more common.^{6c–e}

* To whom all correspondence should be addressed: e-mail gnanou@enscpb.u-bordeaux.fr.

In contrast to anionic polymerization, attempts at developing truly pluricarbocationic initiators of precise functionality were more fruitful so that well-defined stars were obtained from styrene,^{4a,f} isobutylene,^{4b} or alkyl vinyl ethers^{4c,d} and oxazolines.^{4e}

Compared to ionic polymerization techniques, radical processes offer the advantage of being applicable to a wide variety of vinylic monomers and are easier to handle experimentally.⁸ Over the past few years, several families of monomers were demonstrated to polymerize under controlled conditions⁸ by either nitroxide-mediated routes,^{8a-c} ATRP,⁹ reversible addition-fragmentation transfer (RAFT),¹⁰ or some other radical-based methodologies,¹¹ paving the way for the use of these controlled processes in macromolecular engineering. Out of these various mechanisms, ATRP¹² appears as one of the most powerful method for engineering complex macromolecular architectures. ATRP involves the successive transfer of halides or some other functional groups from dormant polymer chain ends to ligated transition metal compounds (Cu, Ru, Fe, Ni), and vice versa, the chains growing between this back and forth transfer when their end is in the free radical form.

Because it affords polymers of predetermined molar masses and narrow polydispersity, ATRP has been used to engineer well-defined miscellaneous block¹³ and graft¹⁴ copolymers as well as hyperbranched¹⁵ and star polymers.¹⁷⁻²⁵

Sawamoto,^{18b} on one hand, and our group,²⁰ on the other, first showed that stars with a high number of arms could be obtained using calixarene derivatized initiators and either Ru(II)/PPh₃ or Cu(I)/bipyridyl as polymerization catalysts. Since then, many groups¹⁷⁻²⁵ have resorted to ATRP to derive star polymers by the core-first method, using several kinds of plurifunctional initiators and activator based on either copper, ruthenium, or nickel halides associated with miscellaneous ligands. Stars constituted of polystyrene, polymethacrylate, or polyacrylate arms whose number ranged from 3 to 12 were synthesized via this route. As each of the systems chosen by the different teams was used under a variety of conditions, it is difficult to identify their specificity and in particular compare their advantages and weaknesses with respect to star synthesis.

In this endeavor, we intend to thoroughly examine the potential of one particular system, namely the one based on copper halides and bipyridyl, when used to derive stars of various chemical nature and functionality.

Starting from commercial calix[*n*]arenes containing 4, 6, and 8 phenolic functions respectively tetra-, hexa- and octafunctional initiators fitted with either bromopropionate or bromoisobutyrate groups were first obtained. The conditions best suited to the synthesis of well-defined multiarm star-shaped polystyrenes, poly(*tert*-butyl acrylate)s, and poly(methyl methacrylate)s were then investigated, using these calix[*n*]arene-based initiators and copper halide associated with bipyridyl as activator.

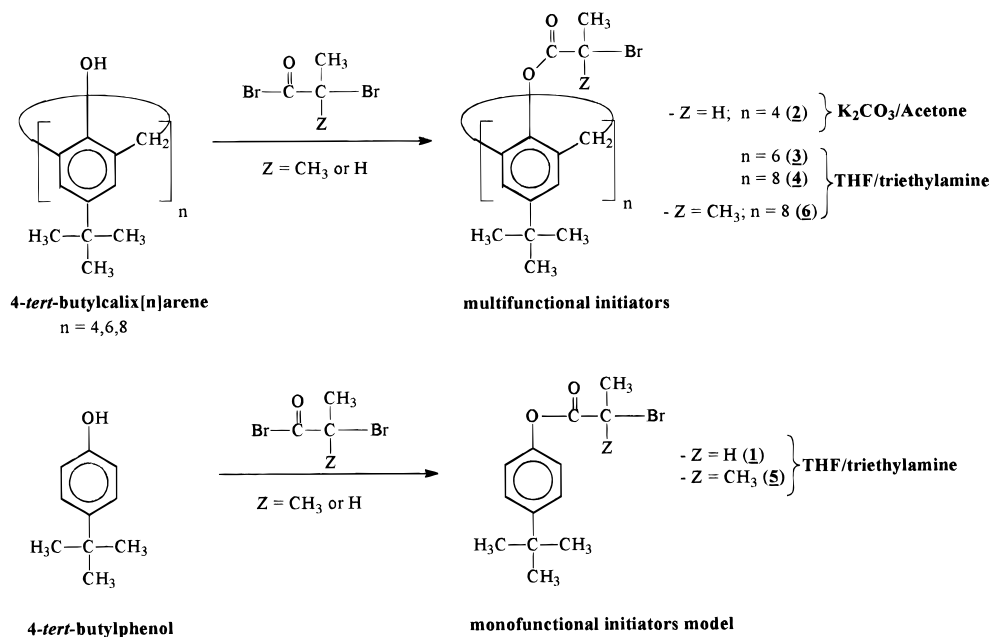
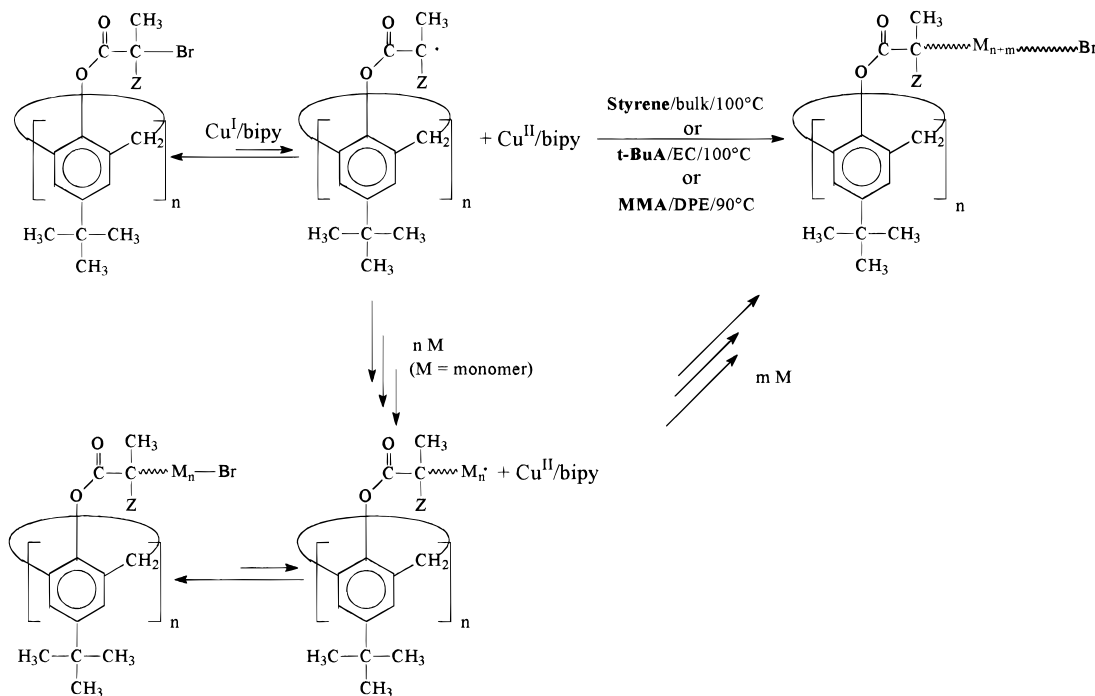
Results and Discussion

1. Synthesis of Initiators of Precise Functionality for the ATRP of Styrene, *tert*-Butyl Acrylate, and Methyl Methacrylate. Prior to the synthesis of star molecules, it was essential to design and prepare perfectly defined initiators that could efficiently trigger the polymerization of the chosen monomers. Because it was shown that alkyl halides containing activated

substituents on their α -carbon, such as carbonyl, could efficiently initiate the polymerization of styrene,²⁶ *tert*-butyl acrylate (*t*-BuA),²⁷ and methyl methacrylate (MMA),²⁸ the latter functional group was introduced on commercially available calix[*n*]arenes.

Calix[*n*]arenes (*n* varying from 4 to 8) are macrocycles obtained from the condensation of para-substituted phenol and formaldehyde.²⁹ The size of the ring of calixarenes can be precisely controlled depending upon the experimental conditions used. The chemical modification of their phenolic functions was extensively investigated, and quite a large number of calix[*n*]arene derivatives were prepared.³⁰ Many of these compounds were shown to host organic molecules, the latter being immobilized through hydrophobic interactions with the aromatic rings. Although frequently employed as synthons in organic chemistry, calixarenes found interest in polymer chemistry only recently.³¹ Kennedy and co-workers^{4b} were the first to utilize modified *tert*-butylcalix[8]arenes as initiators of polymerization. Starting from 5,11,17,23,29,35,41,47-(2-methoxypropyl)-49,50,51,51'-53,54,55,56-octamethoxycalix[8]arene, they cationically grew eight branches of polyisobutylene under "living" conditions and obtained well-defined samples. In a recent addition, Sawamoto and co-workers generated star-shaped PMMA of precise functionality by ATRP using calixarene-based halogenated alkyl esters activated by Ru^{II} catalysts.^{18b} The chemistry of calix[*n*]arenes thus offers the tantalizing possibility of deriving miscellaneous reagents by modification of their phenol functions. The synthesis of novel calix[*n*]arene initiators designed to trigger the Cu^I-activated ATRP of styrene, acrylates, and methacrylates, as depicted in Scheme 1, is described below.

The method followed to prepare the octafunctional initiator **4** was detailed in our previous paper.²⁰ It was readily prepared in one step starting from 4-*tert*-butylcalix[8]arene (TBC) and using 2-bromopropionyl bromide in the presence of triethylamine. Spectroscopic and chromatographic data (two-dimensional cosy ¹³C-¹H NMR spectroscopy, mass spectroscopy, HPLC, etc.) gathered on **4** confirmed the expected structure. In particular, **4** was shown to exist in more than one conformation at room temperature in CDCl₃, its ¹H NMR spectrum exhibiting two different signals for the same hydrogen of CH₃-CH-Br. The replacement of the phenolic protons of TBC by bromopropionate groups not only resulted in a mixture of diastereoisomers but also contributed to rigidify **4**, broadening the signals of its protons in the ¹H NMR spectrum. Using the same experimental conditions as those described for **4**, a hexafunctional **3** and a monofunctional **1** initiators were synthesized from 4-*tert*-butylcalix[6]arene and 4-*tert*-butylphenol, respectively, using 2-bromopropionyl bromide as esterification agent. To obtain the tetrafunctional initiator **2**, the same synthetic strategy could not be applied, the direct esterification of 4-*tert*-butylcalix[4]arene by 2-bromopropionyl bromide failing to give the expected compound because of the insolubility of the calix[4]arene precursor in THF. It is indeed well established that calix[4]arenes exhibit solution behaviors that are different from that of their octa- and hexafunctional counterparts^{30c} because of the strong intramolecular hydrogen bondings occurring in such cyclic compounds. The tetrafunctional initiator could however be obtained by first treating TBC with K₂CO₃ in refluxing acetone and then adding an excess of 2-bromopropionyl bromide.

Scheme 1. Synthesis of Initiators of Various Functionality for ATRP of Styrene, Methyl Methacrylate, and *tert*-Butyl Acrylate, Based on Calix[*n*]arene Chemistry**Scheme 2. Mechanism of ATRP of Styrene, Methyl Methacrylate, and *tert*-Butyl Acrylate**

In Figure 1 are gathered the 1H NMR spectra of the mono- (**1**), tetra- (**2**), hexa- (**3**) and octafunctional (**4**) initiators with the assignment for all the peaks shown. In the case of the tetrafunctional initiator (**2**) the multiplicity of the peaks appearing in the corresponding 1H NMR spectrum is related to the existence of different conformers that hardly interconvert from one to the other.

Since ATRP of MMA requires initiating species that mimic the corresponding dormant chain ends, an initiator containing tertiary alkyl bromide functions was derived. The monofunctional compound **5** and the octafunctional initiator **6** were obtained using 2-bromoisobutyryl bromide as esterification reagent (Scheme 1). The actual structure of the two compounds was

checked through the use of various spectroscopic and chromatographic techniques that all confirmed their high chemical purity and the relevance of the synthetic methodology (Figure 2).

It should be stressed at this stage that the monofunctional bromoesters **1** and **5** were prepared with the view of using them as model initiators and thus establishing the experimental conditions best suited to the controlled polymerization of styrene, *tert*-butyl acrylate, and methyl methacrylate, in the presence of the CuX/2,2'-bipyridyl.

2. Synthesis and Characterization of Linear and Star-Shaped PS Using Mono- (1**) and Multifunctional Initiators (**2**, **3**, and **4**). (a) Octaarmed Polystyrene Stars from Moderate $[M]_0/[Initiator]_0$ Ra-**

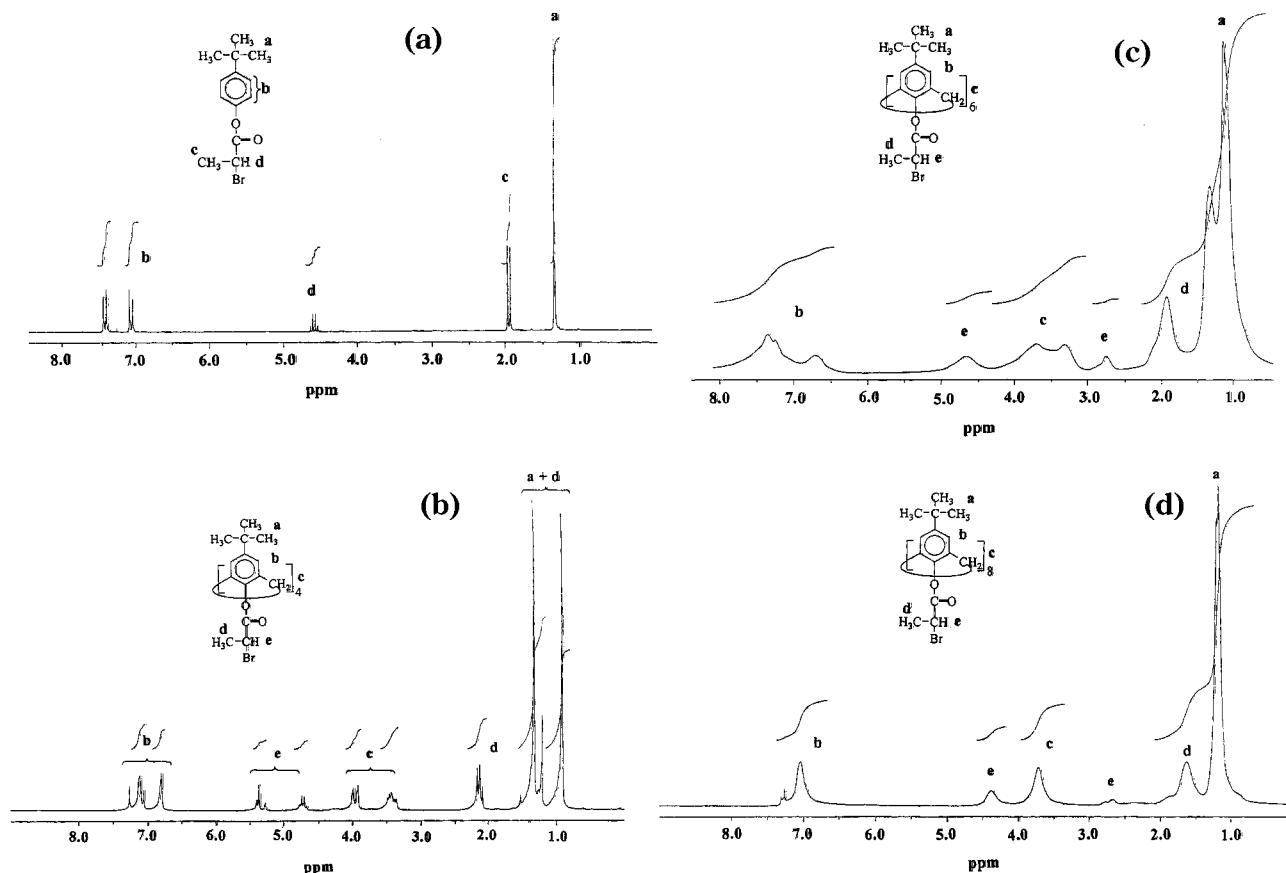


Figure 1. ^1H NMR (CDCl_3) spectra (200 MHz) of mono- and multifunctional initiators containing secondary bromides: (a) monofunctional (**1**), (b) tetrafunctional (**2**), (c) hexafunctional (**3**), and (d) octafunctional (**4**).

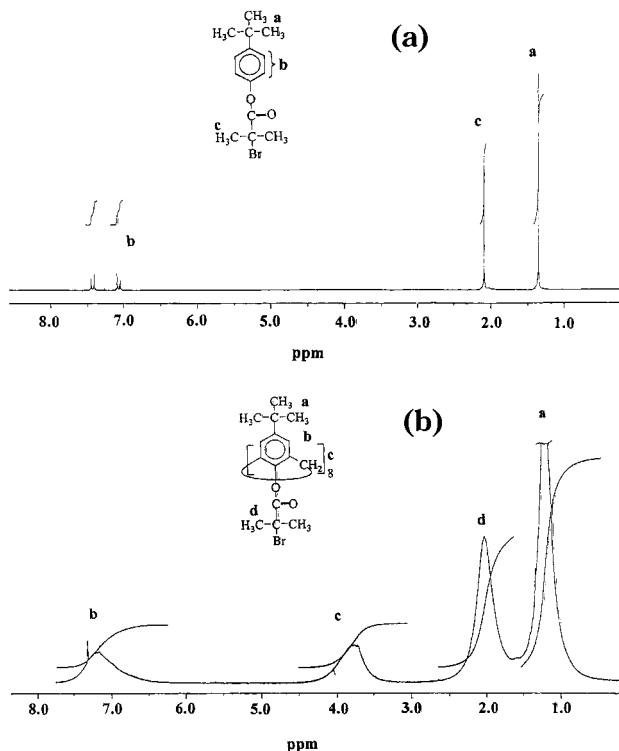


Figure 2. ^1H NMR (CDCl_3) spectra (200 MHz) of mono- and multifunctional initiators containing tertiary bromides: (a) monofunctional (**5**) and (b) octafunctional (**6**).

tios. The bulk polymerization of styrene, using **1** and **4** as initiators and $\text{CuBr}/2,2'$ -bipyridyl as activating system, was already investigated to a certain extent by

Table 1. Bulk Polymerization of Styrene at 100°C , Using Octafunctional Initiator (**4**) and Low $[\text{M}]/[\text{4}]$ Ratios: Evolution of C^* with $[\text{M}]/[\text{4}]$ Ratios and Comparison with $[\text{Star}]^a$

$[\text{M}]/[\text{4}]$	conv (%)	\overline{M}_n LLS (g mol^{-1})	\overline{M}_n theo ^b (g mol^{-1})	$[\text{star}]$ (g L^{-1})	$[C^*]$ (g L^{-1})
935	8.2	10 600	10 300	74.7	191.5
	12.5	15 500	14 100	114	182.6
	17	20 400	19 000	148	181
	20	29 800 ^c	21 800	182	176.8
	26.7	37 200 ^c	28 400	243	83
	41	67 200 ^c	42 400	372	71.9
1500	11.5	25 200	20 500	104.7	167
	17	31 900 ^c	29 000	154.7	149
	21	43 900 ^c	35 200	191.1	92
3000	6	9 700	21 000	54.6	218
	14.6	50 600 ^c	47 900	132.9	66.5
	20	66 700 ^c	64 800	182	63

^a Stoichiometry of $[\text{4}]:[\text{Cu}]:[2,2'\text{-bipyridyl}] = 1:1:3$. ^b \overline{M}_n theo = (conversion $\times [\text{M}]/[\text{4}] \times M_m$) + M_i , where M_m and M_i are the molar masses of styrene and the initiator, respectively. ^c Shoulder in the high molar masses region.

us.²⁰ To obtain octaarmed stars exhibiting molar masses in the range 100 to $300 \times 10^3 \text{ g mol}^{-1}$, $[\text{M}]_0/[\text{4}]_0$ ratios of 935 to 3000 were used at first attempts (Table 1). To our surprise, polystyrene star samples of controlled size and narrow molar mass distribution could be obtained only within a limited range of molar masses ($\overline{M}_n < 60\,000 \text{ g mol}^{-1}$) and conversion ($< 20\%$). Beyond this limit of conversion, irreversible recombination reactions between stars became detectable upon characterization of the corresponding samples by the use of a size exclusion chromatography line equipped with a multi-angle laser light scattering detector (MALLS/SEC).

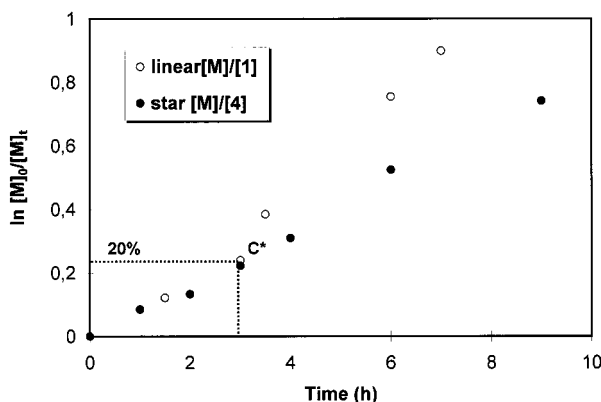


Figure 3. Comparison of the first-order kinetic plots for the bulk polymerization of styrene, using mono- (1) and octafunctional (4) initiators.

Their SEC eluogram indeed revealed the presence of a shoulder in the high molar mass region beside the main peak, suggesting that bimolecular star–star coupling occurred to a nonnegligible extent.

If one considers that the growing arms in octafunctional stars have the same probability of recombination as that of linear chains of similar concentration, the fraction of stars that should be affected by termination should be simply 8 times higher the value for linear species, just because $[RX]_0$ is equal to $8[\text{star}]_0$ ($[RX]_0$ being the initiator concentration). As for their respective kinetics of polymerization, both linear and octafunctional systems should exhibit exactly the same conversion curves, provided the assumption of an equal probability of termination is valid.

A close look at the experimental results shows that the prevailing situation is different from that expected. On the grounds that a $[M]_0/[4]_0$ ratio of 3000 implies a lower concentration of growing polymeric radicals and therefore a lower probability of termination than that corresponding to a ratio of 935, one would have expected a higher monomer conversion for the 3000 ratio experiment than for 935 ratio one before star–star coupling could be detected. As a matter of fact, this reasoning is contradicted by the experimental observations indicating that another factor plays a determining role in the occurrence of star–star coupling, besides the instantaneous concentration of polymeric radicals ($[P^*]$). In this range of $[M]_0/[4]_0$ ratios, the growing octafunctional stars appear more vulnerable to bimolecular termination whenever they cross their critical overlapping concentration (C^*), as if their propensity to recombination were not only controlled by $[P^*]$ but also by $[C^*]$ (with $C^* = 3\bar{M}_w/4\pi R_g^3 N_a$ where \bar{M}_w is the absolute mass average molar mass of the star obtained by light scattering and R_g is the radius of gyration of a linear PS exhibiting the same hydrodynamic volume as that of the star) (Table 1).

Concomitantly to the detection of the star–star coupling above C^* , the kinetics of star polymerization strongly departs from that observed for the monofunctional system of same concentration (Figure 3). This indicates that the octafunctional system undergoes a higher level of termination than does the monofunctional one whenever the stars reach their C^* .

To account for this particular feature, one has to take into consideration the influence of the peculiar shape of the stars on the occurrence of these side reactions. Stars are generally pictured as spherical objects whose

density increases toward the central core and whose arm tips are restricted in their motion to a region that correspond to their external corona. A star-containing reaction medium can thus be portrayed, above C^* , as a collection of overlapping spheres whose respective arms are forced to remain in a close vicinity, unlike the case of linear chain.

Apart from their global shape, the peculiar dynamics of chain growth is another reason that can be put forward to explain a higher tendency of stars to recombine above C^* . Using the rate constants of activation (k_{act}) and deactivation (k_{deact}) determined by Matyjaszewski,³² one can calculate for a given concentration of active species the average lifetime of the corresponding dormant species between two cycles of propagation. For a linear system with 10^{-1} M as initiator concentration, one respectively obtains 22 and 1.8×10^{-5} s for the average rest and propagation times, leading to a ratio of 8.2×10^{-7} . In the case of octafunctional systems, that can also be identified with an assembly of eight chains, the evaluation of the maximum time ($\tau_{\text{act},8}$) eight arms can stay active before anyone of them is deactivated and the smallest possible time ($\tau_{\text{rest},8}$) a collection of eight chains may altogether remain dormant yields totally different values. $\tau_{\text{act},8}$ merely corresponds to 8 times the value obtained for linear chains (1.44×10^{-4} s); as for $\tau_{\text{rest},8}$, it can be deduced by dividing $\tau_{\text{rest},8}$ for monofunctional chains by 2^{8-1} , considering that $\tau_{\text{rest},2}$ for two chains is merely $22/2^{2-1}$, a set of three such chains $22/2^{3-1}$, etc. Dividing $\tau_{\text{act},8}$ by $\tau_{\text{rest},8}$ yields a ratio of 8.5×10^{-4} , which is 3 orders of magnitude higher than the value found for the monofunctional system.

The particular topology of star-shaped molecules—and its influence on the motion of reactive ends—as well as the dynamics of activation/deactivation of multifunctional systems may well be responsible for the behavior observed above C^* , that is a higher extent of termination, due to a higher rate of termination ($k_{t,\text{star}}$) than that corresponding to the monofunctional system.

(b) Octaarmed Polystyrene Stars from Large $[M]_0/[\text{Initiator}]_0$ Ratios. In an attempt to overcome the limitations due to star–star coupling, a novel series of experiments with much higher $[M]/[4]$ ratios (6000–20 000) was carried out. By lowering the instantaneous concentration of growing radical, one can indeed expect to decrease the probability of termination and obtain well-defined stars of much higher molar masses. Under these conditions well-defined octaarmed stars could be easily obtained up to 600 000 g mol⁻¹, and no star–star coupling could be detected even for a conversion as high as 25% that is well above the C^* of the samples considered (Table 2).

Table 2. Bulk Polymerization of Styrene at 100 °C, Using 4 as Octafunctional Initiator and High $[M]/[4]$ Ratios^a

$[M]/[4]$	conv (%)	\bar{M}_n LLS (g mol ⁻¹)	\bar{M}_n theo ^b (g mol ⁻¹)	$[\text{star}]$ (g L ⁻¹)	$[C^*]$ (g L ⁻¹)
6 000	12.5 (15 h)	84 000	80 400	109.4	22.8
	19.5 (20 h)	155 000	146 000	170.6	48.8
12 000	18 (27 h)	275 000	230 000	157.5	8.6
	25 (38 h)	487 000	450 000	218.7	5.1
20 000	22 (40 h)	460 000 ^c	458 000	192.5	4.5
		500 000			
		580 000 ^c			

^a Stoichiometry of $[4]:[\text{Cu}]:[2,2'\text{bipyridyl}] = 1:1:3$. ^b \bar{M}_n theo = (conversion $\times [M]/[4] \times M_m$) + M_i , where M_m and M_i are the molar masses of styrene and the initiator, respectively. ^c After cyclohexane extraction.

However, the use of such large $[M]/[I]$ ratios occasioned a minor drawback that was the contamination of the PS stars with linear chains independently produced by the thermal self-initiation of styrene. To isolate pure star samples, it was necessary to carry out a last step of fractionation. It should be stressed that the amount of these linear chains never exceeded 10% in weight, and their presence could be detected only after 15 h of reaction, the peak due to linear species in the SEC eluograms becoming more prominent with the duration of polymerization. When taking the ratio of molar masses corresponding respectively to linear and star species, one systematically obtained values revolving 8, signifying that the linear chains detected were created from the very beginning of polymerization by the thermal process and grew at the same rate as that of the star arms. Even though the thermal generation of linear chains in nonnegligible amounts may appear at first glance as a drawback—requiring a fractionation step—their presence in the reaction medium seems to prevent stars from mutually coupling (besides the lower concentration of polymeric radicals) upon crossing C^* . This beneficial effect can be accounted for using the following arguments. Because they are surrounded by linear chains that can in particular penetrate their external corona, stars with their spherical shape should have less opportunity to extensively overlap and to self-couple. As for the coupling between the linear chains and stars, it certainly occurred, giving rise to stars with only seven active sites, but the novel species formed could not be detected by any of the techniques used.

(c) Tetra- and Hexaarmed Polystyrene Stars from 2 and 3 as Initiators. After the preparation of octaarmed PS stars, the synthesis of hexa- and tetraarmed PS stars was attempted starting from the tetra- and hexafunctional initiators **2** and **3**, respectively. The results of the bulk polymerization of styrene using **2** and **3** as initiators in the presence of CuBr/2,2'-bipyridyl at 100 °C are listed in Table 3.

It can be seen from Figure 4 that the ATRP of styrene exhibits approximately the same kinetics in this range of $[M]/[I]$ ratios, for the hexa- and tetrafunctional initiators, the rate of polymerization being mainly governed by the concentration of polymeric radicals. The kinetic plots show a first-order rate of propagation with respect to the monomer concentration, meaning that the concentration of the growing radicals remained constant during the polymerization.

With the hexafunctional system, the molar mass control was retained up to 20–25% monomer conver-

Table 3. Bulk Polymerization of Styrene at 100 °C, Using 2 and 3 as Tetra- and Hexafunctional Initiators^a

<i>F</i>	$[M]/[I]$	time (h)	conv (%)	\overline{M}_n SEC (g mol ⁻¹)	\overline{M}_n LLS (g mol ⁻¹)	\overline{M}_n theo ^b (g mol ⁻¹)	PDI
6	1125	5	22.6	25 800	33 900	28 200	1.18
6	1125	7	32.5	37 000	54 000 ^c	38 100	1.17
6	2250	10	20	40 300	48 600	53 200	1.12
6	9000	30	22.5	83 500	210 600	207 800	1.20
6	13000	38	23	243 400	433 000 ^d	311 000	1.15
4	750	7	35.8	27 100	29 100	31 200	1.19
4	750	9	48.9	33 200	39 700	39 300	1.16
4	1500	16	26	33 400	40 000	41 700	1.16
4	2000	37	48.1	60 200	101 200	90 000	1.13

^a Stoichiometry of $[I]:[Cu]:[2,2'\text{-bipyridyl}] = 1:1:3$. ^b \overline{M}_n theo = (conversion $\times [M]/[I] \times M_n$) + M_i , where M_n and M_i are the molar masses of styrene and the initiator, respectively. ^c Shoulder in the high molar mass region. ^d After cyclohexane extraction.

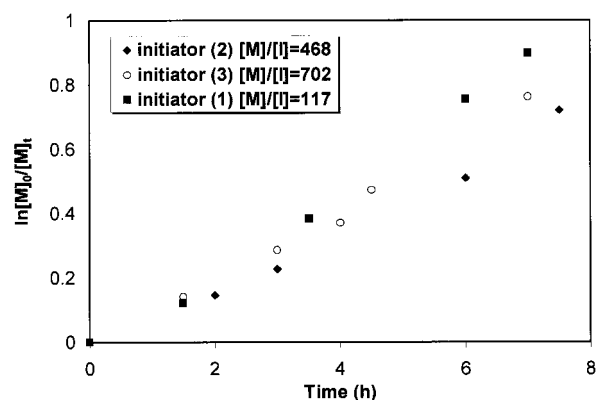


Figure 4. First-order kinetic plots for the bulk polymerization of styrene, using mono- (**1**), tetra- (**2**), and hexafunctional initiators (**3**) at 100 °C.

Table 4. Bulk Polymerization of Styrene at 100 °C, Using 2 and 3 as Tetra- and Hexafunctional Initiators: Evolution of C^* with $[M]/[I]$ Ratios and Comparison with $[Star]$

<i>F</i>	$[M]/[I]$	conv (%)	\overline{M}_n LLS (g mol ⁻¹)	$[star]$ (g L ⁻¹)	$[C^*]$ (g L ⁻¹)
6	702	13.3	13 600	121	251.1
6	702	25	26 000	227.5	107.6
6	702	31 ^a	30 000	282.1	102.5
6	2250	12	33 000	109.2	114
6	2250	20	53 200	182	69.8
6	2250	27.5 ^a	95 000	250.2	49.7
4	468	20.4	10 900	185.7	320.4
4	468	40	19 000	364	116.7
4	468	51.4	29 600	467.8	94.5
4	1500	15.7	24 200	142.9	151.1
4	1500	21.3	35 000	193.8	89.3
4	1500	26	40 000	236.6	73.6

^a Shoulder in the high molar mass region.

sion, the experimental \overline{M}_n values—determined by MALLS/SEC—matching quite well the targeted ones. Beyond this range of conversion, star–star coupling became detectable, and the molar mass control was then totally elusive.

As for the tetrafunctional system, the occurrence of side coupling reactions was detectable at much higher monomer conversion. Indeed, the appearance of a shoulder in the MALLS/SEC traces due to star–star coupling was observed only after crossing 50% monomer conversion, whatever the ratios of the monomer to the initiator used.

As shown in Table 4, both tetra- and hexafunctional stars can extensively overlap above C^* without being subjected to intermolecular coupling. Their lower functionality as compared to the octafunctional one leaves indeed less chances for two independently growing branches to meet and recombine, the probability for tetra- and hexafunctional stars to get coupled being respectively one-half and two-thirds that experienced by octafunctional samples.

The fact that the various samples obtained were all completely soluble with no cross-linked material even at high conversion means that the overall concentration of growing radicals remained very low throughout the polymerization process. This means also that samples of very high molar masses, free of any coupled species of higher functionality, could be obtained provided the initial feed ratio $[M]/[I]$ is high enough.

The use of such $[M]/[I]$ ratios in the case of hexaarmed stars did result in a dramatic decrease of the rate of

polymerization (dilution effect)—as previously noticed—and requested longer polymerization times. Under such conditions, self-thermal polymerization of styrene that operated independently of the star growth generated enough linear polymer chains to be detected by SEC. The aliquots removed from the reaction after the onset of the polymerization indeed showed the presence of an additional low molar mass peak in the MALLS/SEC. A value of 6 was found for the ratio of the molar mass ascribed to the two peaks in the case of hexafunctional system. Pure hexaarmed stars were then separated from the linear contaminants by selective extraction of the latter in cyclohexane. Owing to their functionality and their lower probability to undergo bimolecular coupling, tetraarmed stars could be obtained without resorting to high $[M]/[I]$ ratios. As a result, such tetraarmed stars could grow at a rate high enough to prevent their contamination by linear chains generated by the thermal process.

Apart from their characterization by MALLS/SEC, multiarmed stars of low molar masses ($\overline{M}_n < 3000$ g mol⁻¹ per branch) were subjected to analysis by ¹H NMR. Their ¹H NMR spectra exhibited a signal at 4.5 ppm assignable to the secondary bromine end group ($-\text{CH}_2\text{CH}(\text{C}_6\text{H}_5)\text{Br}$), while the signal corresponding to the methine proton of the initiator (at 4.3 ppm) completely vanished, indicating a quantitative initiation. To check the accurate functionality of the various stars obtained, the following experiments were purposely designed and carried out.

(d) Determination of the Functionality of Polystyrene Star Using a Mixture of Mono- and Multifunctional Initiators. On one hand, a series of bulk experiments were performed using equimolar amounts of monofunctional and either of the multifunctional initiators **3** or **4** previously described. Because the kinetics of mono- and multifunctional systems are quite similar until irreversible star–star couplings become detectable (as previously demonstrated), each arm of the stars synthesized under such conditions should exhibit the same molar mass as that of the linear chain concomitantly formed.²⁰ This reasoning was also followed by Matyjaszewski in a recent contribution.^{17c} Different $[M]/[I]$ ratios were used—with $[I] = [\mathbf{1}] + [\mathbf{3}]$ or $[\mathbf{4}]$ —so as to obtain mixtures of stars and linear species in a broad range of molar masses. As in the attempts at generating pure PS stars, these experiments were discontinued at relative low monomer conversion so as to retain the control of the star structure. Typical MALLS/SEC traces of the materials obtained with the hexafunctional system are shown in Figure 5; two peaks can be seen, as expected: the peak in the high molar mass region can be assigned to the star whereas the one appearing at higher elution volumes is obviously due to linear PS chains.

It is worth mentioning that the data arising from the refractometric detector (RI) are directly proportional to the concentration of the populations eluted, whereas those drawn from light scattering are proportional to MC (where M is the absolute molar mass and C the concentration of the population considered). Thus, equimolar amounts—in one pot—of mono- and multifunctional initiators should give rise to two distinct populations of same concentration, as evidenced in the RI/SEC trace. In the case of the tetrafunctional system, the distinction between the peaks due to the linear and star species was not as marked as it was for the hexa-

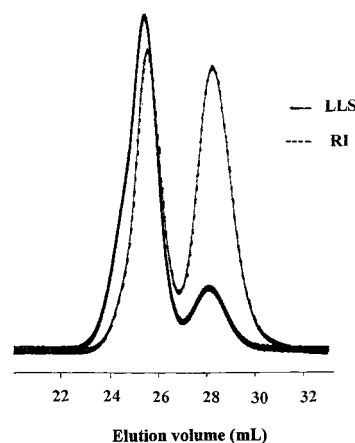


Figure 5. SEC traces (LLS and RI detectors) of a mixture of linear and star polystyrenes, obtained by using equimolar amounts of **1** and **3** as initiators.

Table 5. Determination of the Actual Functionality of Polystyrene Stars

$f(\text{theo})$	\overline{M}_n LLS star (g mol ⁻¹)	\overline{M}_n SEC linear (g mol ⁻¹)	$f(\text{calcd})^a$
8	52 000 ^b	6 400	8.1
8	123 000 ^b	16 000	7.7
8	340 000 ^c	43 000	7.9
6	36 500 ^b	6 000	6.1
6	83 800 ^c	14 200	5.9
6	127 500 ^b	21 300	5.9
4	70 000 ^c	18 600	3.8
4	101 200 ^c	26 100	3.9

^a $f = \overline{M}_n \text{ star (LLS)} / \overline{M}_n \text{ linear (SEC)}$. ^b Mixture of mono- and multifunctional initiators. ^c Cleavage of the ester function under basic conditions.

and octafunctional systems. This is due to the fact that both tetraarmed PS stars and linear PS chains formed may exhibit similar hydrodynamic volumes in the range of the molar masses targeted. By taking the ratio of the \overline{M}_n of the star to that of the linear polymers, the average functionality of the samples obtained from initiators **3** and **4** could be estimated. This ratio was found to be close to the theoretical value of 6 and 8, respectively, thus confirming the presence of a precise controlled number of branches connected to the calixarene core (Table 5).

(e) Characterization of Polystyrene Stars: Hydrolysis of Their Arms. Taking advantage of the presence of ester links between the arms and the core, we tried to cleave this linkage under basic conditions and indirectly determine the functionality of the star synthesized. Core destruction was indeed reported earlier as a useful method to determine the number of branches in a star structure.^{4b,16,18–21,25} Our star polymers were thus hydrolyzed using KOH in a mixture of THF and ethanol, and the resulting polymers isolated after hydrolysis were characterized by SEC. The ratio of the molar mass of the stars with that of the hydrolyzed arms gave an idea of the quality of the stars prepared. Typical SEC traces of the star precursor and of the surviving arms are shown in Figure 6.

Of particular relevance was the fact that these PS hydrolyzed arms all exhibited a monomodal distribution and a polydispersity index close to 1; there was no evidence of higher molar mass byproduct. Moreover, the \overline{M}_n 's of these linear PS were found to be $1/4$, $1/6$, and $1/8$ of those corresponding to the precursor tetra-, hexa-, and

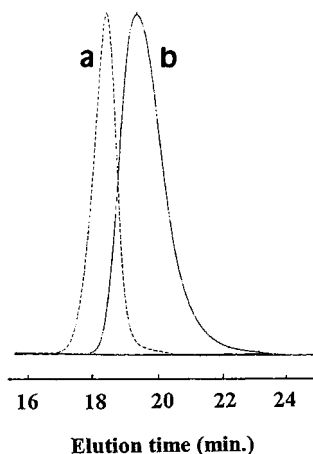


Figure 6. SEC traces (RI detector) (a) before and (b) after hydrolysis of the ester functions of an octaarmed PS star.

octafunctional stars, respectively. This means that the calixarene core acted as an efficient multifunctional initiator, all its bromopropionate functions giving rise to branches of PS stars.

Ill-defined stars containing products of bimolecular coupling were also subjected to hydrolysis; the SEC traces of the hydrolyzed products exhibited a bimodal distribution of the molar masses. As the high molar mass peak approximately corresponded to twice that calculated from the main peak, the comparison of their respective surfaces gave an indication of the extent of star molecules that underwent bimolecular coupling.

3. Synthesis and Characterization of Linear and Star-Shaped Poly(*tert*-butyl acrylate)s Using Mono-(1) and Octafunctional Initiators (4). Bromopropionate groups were chosen to initiate the ATRP of acrylates on the grounds that their structure is similar to that of the growing polymer chain end in its dormant form. Indeed, with this kind of initiator, a variety of alkyl acrylates (with primary, secondary, or tertiary alkyl group) were successfully polymerized by ATRP using the conventional CuX/2,2'-bipyridyl system.

There are only a few reports²⁷ on the ATRP of *tert*-butyl acrylate (*t*-BuA) using CuX/2,2'-bipyridyl or CuX/*N,N,N',N'',N'''*-pentamethyldiethylenetriamine systems, and synthesis of star-shaped poly(*tert*-butyl acrylate)s was recently described.^{17c–27a} This monomer is usually polymerized under “living” anionic conditions,³³ and the resulting poly(*t*-BuA) generally serves as precursor to well-defined poly(acrylic acid), the latter being isolated after removal of the *tert*-butyl groups of poly(*t*-BuA) under acidic conditions. Despite the economical importance of this hydrophilic polymer that finds many applications in the domain of coating and biomaterials, the corresponding monomer that is acrylic acid could not be polymerized via either nitroxide-mediated route or ATRP because of their intolerance to carboxylic functions. RAFT¹⁰ is a more recent method that allows the polymerization of acrylic acid under controlled conditions. Until recently, the best option to obtain easily poly(acrylic acid) samples of controlled size was to polymerize *t*-BuA by ATRP and subsequently hydrolyze their *tert*-butyl groups.

The conditions described by Matyjaszewski et al.³⁴ for the ATRP of *n*-butyl acrylate were applied to polymerize *t*-BuA, **1** and **4** being used as initiators for this purpose. The conversion curve of the ATRP of *t*-BuA at 100 °C using **1** as monofunctional model and CuBr/2,2'-bipy-

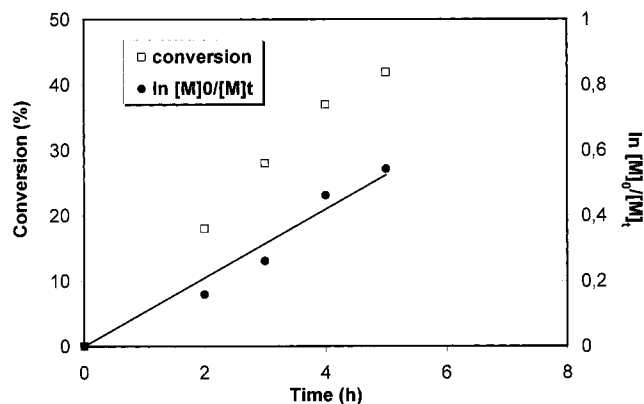


Figure 7. First-order kinetic plot for the polymerization of *tert*-butyl acrylate, using **1** as monofunctional initiator at 100 °C with $[M]/[1] = 100$.

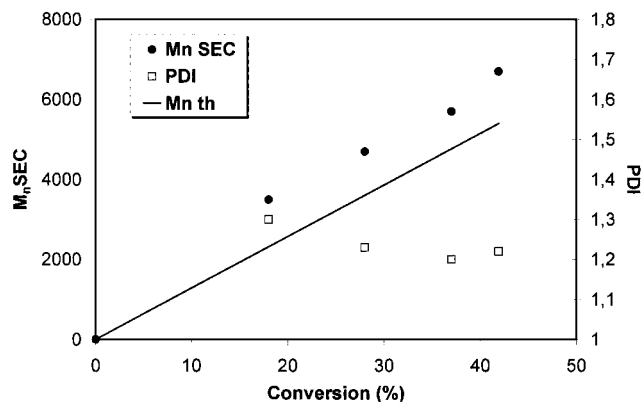


Figure 8. Evolution of molar masses and molar mass distributions with monomer conversion for the ATRP of *tert*-butyl acrylate at 100 °C, using **1** as initiator with $[M]/[1] = 100$.

ridyl as catalyst in the presence of ethylene carbonate (10% in volume relative to *t*-BuA) is plotted in Figure 7. The use of ethylene carbonate as additive was indeed found essential to bring about the controlled polymerization of alkyl acrylates in the presence of substituted bipyridyl.³⁴

The linear character of the conversion plot indicates that the concentration in active species remained constant throughout the course of the polymerization, regardless of the initial concentration in **1**. M_n values were found to vary linearly with conversion, revealing a negligible contribution of transfer reactions (Figure 8).

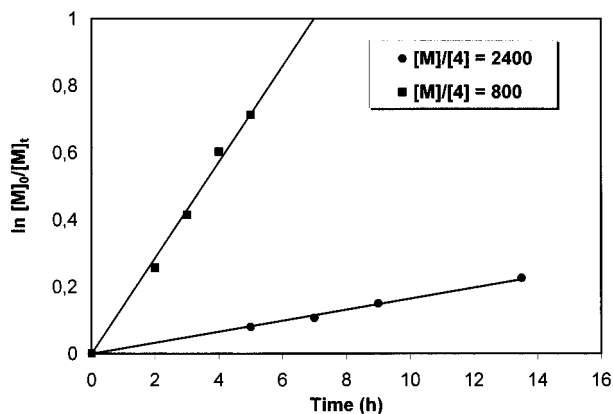
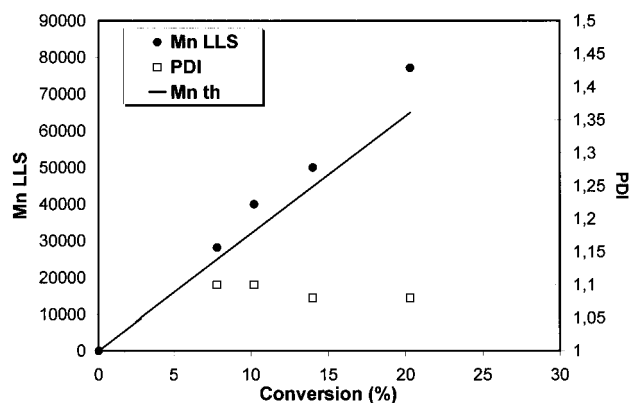
However, the experimental values determined by SEC appeared higher than the theoretical ones. This feature was also observed by Matyjaszewski,²⁷ who attributed this discrepancy between experimental and targeted molar masses to the inadequacy of the calibration of SEC columns—usually calibrated with linear PS standards—rather than to the incompleteness of the initiation reaction. The poly(*t*-BuA)s obtained all exhibited a low polydispersity, and their SEC traces were found monomodal. These results confirm that the bromoester **1** is an efficient initiator for the ATRP of *t*-BuA in the presence of ethylene carbonate and CuBr/2,2'-bipyridyl as activating agent.

After establishing the conditions the best suited to bring about the controlled polymerization of *t*-BuA with the monofunctional model **1** as initiator, its octafunctional analogue **4** was used to grow star carrying

Table 6. Polymerization of *tert*-Butyl Acrylate at 100 °C, Using **4** as Octafunctional Initiator^a

[M]/[4]	time (h)	conv (%)	\overline{M}_n SEC (g mol ⁻¹)	\overline{M}_n LLS (g mol ⁻¹)	\overline{M}_n theo ^b (g mol ⁻¹)	PDI
800	2	22.6	21 700	31 800	25 500	1.10
800	3	33.9	27 700	55 000	37 000	1.13
800	4	45.3	36 100	48 800	50 000	1.10
800	5	51	42 800	65 000	55 000	1.10
2400	5	7.8	21 500	28 200	26 400	1.08
2400	9	14	37 000	43 200	50 000	1.08
2400	13.5	20.3	58 800	77 200	64 800	1.08

^a Stoichiometry of [**4**]:[Cu]:[2,2'-bipyridyl] = 1:1:2. ^b \overline{M}_n theo = (conversion × [M]/[**4**] × \overline{M}_n) + \overline{M}_i , where \overline{M}_n and \overline{M}_i are the molar masses of *tert*-butyl acrylate and the initiator, respectively.

**Figure 9.** First-order kinetic plot for the polymerization of *tert*-butyl acrylate, using **4** as octafunctional initiator at 100 °C with [M]/[**4**] = 800 and 2400.**Figure 10.** Evolution of molar masses and molar mass distributions with monomer conversion for the ATRP of *tert*-butyl acrylate, using **4** as initiator at 100 °C with [M]/[**4**] = 2400.

precisely eight branches of poly(*t*-BuA) under the same experimental conditions. Two different ratios of [M]/[**4**] were chosen to obtain samples of different molar masses, on one hand, and to investigate the occurrence of star–star coupling reactions as a function of [**4**], on the other. The results are listed in Table 6 and plotted in Figures 9 and 10.

The plot of $\ln[M]_0/[M]_t$ as a function of time reveals a linear variation for both [M]/[**4**] ratios and, as expected, the higher the initial [M]/[**4**] ratio the slower the rate of polymerization. The conversion curve also shows that there is no loss of active species during the course of the polymerization process. It is worth mentioning that, whatever the molar mass targeted, the experimentally determined \overline{M}_n values were found in close agreement to the expected ones, the latter being derived from

Table 7. Determination of the Actual Functionality of Poly(*tert*-butyl acrylate) Stars

$f(\text{theo})$	\overline{M}_n LLS star (g mol ⁻¹)	\overline{M}_n SEC linear (g mol ⁻¹)	$f(\text{calcd})^a$
8	85 000	11 800	7.2
8	95 300	13 500	7.1

^a $f = \overline{M}_n \text{ star (LLS)} / \overline{M}_n \text{ linear (SEC)}$.

[M]/[**4**] ratios targeted and the conversion obtained. The MALLS/SEC traces of the samples systematically exhibited a unimodal and perfectly symmetrical distribution, and in sharp contrast with the synthesis of star-shaped polystyrene, they did not reveal the presence of a side population in the high molar mass region due to star–star coupling. Such species, if they were formed, would have been detected by MALLS/SEC; this indicates that star–star coupling, if it cannot be totally ruled out, occurred to a negligible extent because ATRP of *t*-BuA implies very small concentration of radicals in this range of [M]/[**4**] ratios.

The differences found in the synthesis of PS and poly(*t*-BuA) stars actually stem from the contrasted values taken by the equilibrium constant K_{eq} ($K_{eq} = k_a/k_d$) for the two monomers. This variation of K_{eq} from one class of monomer to another one merely reflects the better propensity of the Cu^{II}/bipyridyl complex to deactivate polyacrylic radicals than polystyryl ones.^{8b} For instance, K_{eq} values for the ATRP of styrene at 110 °C, that of methyl methacrylate and methyl acrylate at 90 °C using CuBr/dinonylbipyridyl, were estimated in the following order: $K_{eq,MMA} > K_{eq,styrene} > K_{eq,MA}$.

As a result, the polymerization of *t*-BuA using **4** as initiator could be carried out to high conversion and well above the C^* of the samples without contaminating octaarmed stars with species of higher functionality, despite the use of relatively high [M]/[**4**] ratios.

To better demonstrate that these poly(*t*-BuA) stars indeed exhibited a well-defined character, the eight ester functions linking their arms to the central core were cleaved under basic conditions, and the produced linear poly(*t*-BuA) chains were analyzed. At this stage, it was crucial to selectively hydrolyze the eight phenyl ester linkages without damaging the *tert*-butyl ester groups of the repeating units. This was readily achieved by treating the star molecule in refluxing THF for a short period of reaction (few minutes) in the presence of KOH. The characterization by ¹H NMR of the polymer recovered after this basic treatment clearly showed that the *tert*-butyl ester groups in poly(*t*-BuA)s were entirely preserved with no sign of their cleavage into carboxylic functions. The same sample exhibited a significant decrease of its molar mass as compared with that of its uncleaved precursor, a ratio of 1 to 8 being obtained between the two sets of molar masses by MALLS/SEC (Table 7).

In addition to this feature, the SEC traces of the hydrolyzed polymers were found unimodal, attesting to the strictly octafunctional character of the poly(*t*-BuA) stars prepared. It has to be mentioned that the possibility to prepare star-shaped poly(acrylic acid) by selective cleavage of the *tert*-butyl group was not investigated.

4. Synthesis and Characterization of Linear and Star-Shaped Poly(methyl methacrylate)s Using Mono- (5**) and Octafunctional Initiators (**6**).** The ATRP of MMA was reported to be controlled in the presence of a variety of activated halides and of metal

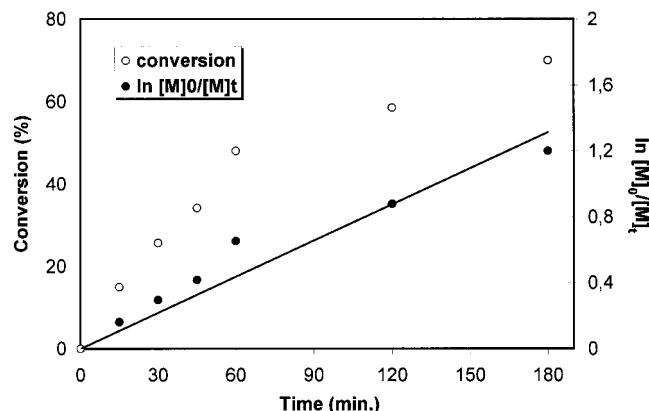


Figure 11. First-order kinetic plot for the polymerization of methyl methacrylate, using **5** as monofunctional initiator at 90 °C with $[M]/[5] = 300$.

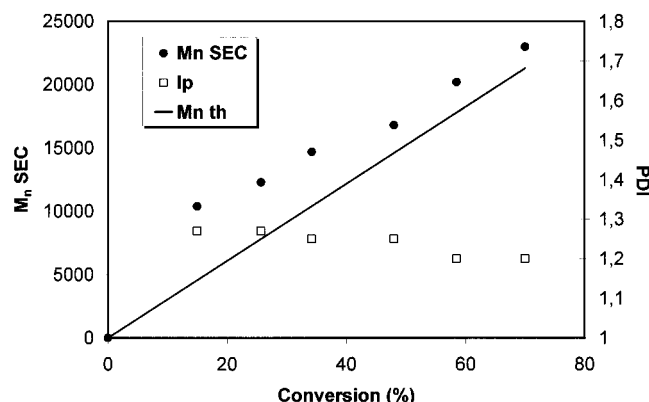


Figure 12. Evolution of molar masses and molar mass distributions with monomer conversion for the ATRP of methyl methacrylate at 90 °C, using **5** as initiator with $[M]/[5] = 300$.

catalysts such as $\text{NiBr}_2(\text{PPh}_3)_2$ ³⁵ or $\text{RhBr}_2(\text{PPh}_3)_2$ ³⁶ used as initiators and activators, respectively.

Linear PMMAs of predetermined molar mass ($10\,000$ – $180\,000\text{ g mol}^{-1}$)^{8h} were also prepared by ATRP mediated by copper salts systems. The process was generally conducted at 90 °C in 50% diphenyl ether solution with preferentially CuCl/bipyridyl —rather than CuBr —as activating system. Various initiators (2-bromomethyl malonate and benzyl chloride used by Matyjaszewski²⁸) were found to function adequately, but the best ones are those based on arenesulfonyl halides developed by Percec;³⁷ multifunctional sulfonyl chlorides were even shown to be very efficient to synthesize PS and PMMA stars up to high conversion.^{23a}

Polymerizing MMA by ATRP using an initiator of the same family as that employed for styrene and *t*-BuA requires that an activated alkyl tertiary halide such as β -bromoester be introduced in the calixarene-based compounds. In analogy with the previous sections, a monofunctional model (**5**) was first prepared and used with a view of establishing the conditions the best suited to control the ATRP of MMA before these conditions could be applied to the octafunctional system (**6**).

Figures 11 and 12 showed the results obtained with **5** as initiator. As clearly indicated, all aliquots sampled out throughout the polymerization process exhibit a monomodal distribution of molar masses and polydispersities revolving around 1.25. Although their \overline{M}_n values increase linearly with the monomer conversion, it can be noted that the experimental values depart from the theoretical line, especially in the low molar mass

Table 8. Polymerization of Methyl Methacrylate at 90 °C, Using **6** as Octafunctional Initiator^a

$[M]/[6]$	time (min)	conv (%)	\overline{M}_n SEC (g mol ⁻¹)	\overline{M}_n LLS (g mol ⁻¹)	\overline{M}_n theo ^b (g mol ⁻¹)	PDI
2400	15	15	22 200	36 500	38 500	1.13
2400	30	38.4	59 300	118 000 ^c	94 800	1.22
4000	20	12.5	30 000	51 700	52 800	1.13
4000	40	27	78 000	146 500 ^c	110 600	1.16
5600	45	14	50 500	77 300	81 000	1.14
5600	60	25	90 900	166 000 ^c	140 300	1.13
11200	120	14.3	80 900	154 000	160 000	1.15
16000	255	14.3	122 000	232 300	230 200	1.08

^a Stoichiometry of $[6]:[\text{Cu}]:[2,2'\text{-bipyridyl}] = 1:1:2$. ^b \overline{M}_n theo = (conversion $\times [M]/[6] \times \overline{M}_m$) + \overline{M}_i , where \overline{M}_m and \overline{M}_i are the molar masses of methyl methacrylate and the initiator, respectively.

^c Shoulder in the high molar mass region.

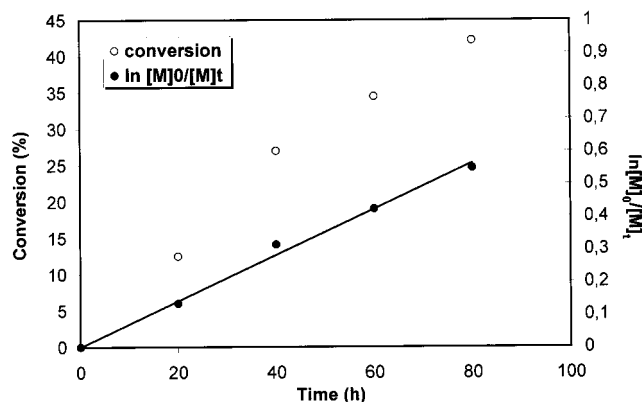


Figure 13. First-order kinetic plot for the polymerization of methyl methacrylate, using octafunctional initiator **6** at 90 °C with $[M]/[6] = 4000$.

region, indicating a slow initiation (or a slow interconversion between active and dormant species). Using their ruthenium-based system and a *tert*-butylphenol derived initiator containing an activated chloride, Sawamoto and co-workers¹⁸ also made the same observation. They attributed the discrepancy between expected and actual values to a slow initiation rather than to the use of PS standard for the calibration of their SEC columns. In the event of a slow initiation, polydispersity index should decrease with the conversion which is actually observed as shown in Figure 12.

Thus, the use of the same experimental conditions for the synthesis of octafunctional PMMA stars should yield star species whose arms might exhibit some fluctuation in their size. In Table 8 are shown the results obtained with the octafunctional initiator **6** used in the presence of CuCl/bipyridyl at 90 °C in 50% diphenyl ether solution.

The samples were characterized by SEC using concomitant UV and refractometric detection. The UV trace that is mainly due to the absorbing calixarene-based core was found to perfectly coincide with that originating from the refractometric detection. This feature simply mirrors the well-defined character of the PMMA stars formed and their homogeneity in functionality. As for the kinetics of polymerization, they exhibited for the three $[M]/[I]$ ratios employed a first-order dependence of the rate of propagation on the monomer concentration (Figure 13).

Similar to the case of the PS stars, the polymerization had to be discontinued at relatively low conversion in monomer in order to obtain truly octafunctional PMMA stars samples whose \overline{M}_n match the targeted values

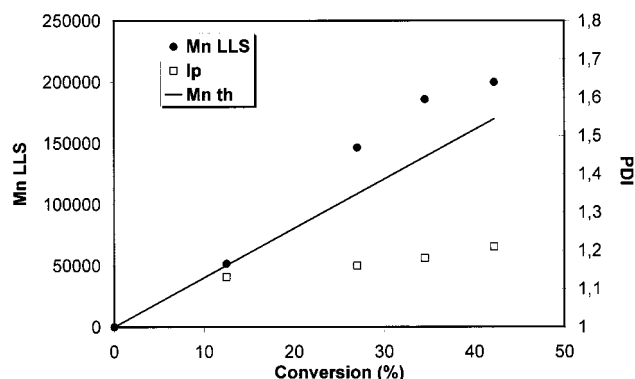


Figure 14. Evolution of molar masses and molar mass distributions with monomer conversion for the ATRP of methyl methacrylate, using **6** as initiator at 90 °C with $[M]/[6] = 4000$.

(Figure 14). Indeed, beyond a threshold of conversion that revolves around 20–25%, a shoulder could be detected in the high molar mass side of the MALLS/SEC traces of the PMMA stars. For the PS stars, this shoulder was attributed to the coupling of two growing arms that resulted in the formation of star species of higher functionality than 8. As K_{eq} in the ATRP of MMA is known to be larger at 90 °C than that of styrene at 110 °C, the occurrence of star–star coupling is not surprising. Very likely, this higher K_{eq} value might reflect the lesser aptitude of Cu^{II} /bipyridyl to deactivate tertiary PMMA radicals than secondary polystyryl radical.

Even though the ATRP of MMA is associated with a larger K_{eq} value than styrene, the probability for two stars to couple should be nonetheless lower than for PS stars just because k_p/k_t is higher for the former monomer.⁷ The fact that PMMA radicals tend to disproportionate should not prevent bimolecular termination from occurring since the unsaturated chain end may be consumed by copolymerization.

Therefore, for similar $[M]/[I]$ ratios, the polymerization could be carried out to higher conversion in the case of MMA—as compared to the case of ATRP of styrene—before the star–star coupling phenomenon could be detected.

Following the same strategy as that adopted for the preparation of PS stars, PMMA stars of higher molar mass could be obtained using large $[M]/[I]$ ratios and restricting the polymerization to low conversion. This effectively afforded well-defined octafunctional stars with rather large arm size of 10 000 g mol^{−1}.

Another way to reduce the extent of termination in the course of the synthesis of PMMA stars was proposed by Percec et al.:^{23a} these authors resorted to multifunctional sulfonyl chlorides as initiators that are known to give rise to a quantitative initiation with much faster rate than that of propagation. In these conditions, well-defined PPMA stars up to high conversion could be obtained.

To check their actual functionality, the samples obtained were subjected to cleavage of their core, using the conditions previously described. The completeness of the cleavage process was first confirmed by ¹H NMR and SEC which showed that the resulting polymer underwent a significant decrease of its molar mass, as compared with that of the star precursor. As shown in Table 9, the \bar{M}_n values of PMMA stars and those of the hydrolyzed products give a ratio that revolves around the expected value of 8.

Table 9. Determination of the Actual Functionality of Poly(methyl methacrylate) Stars

$f(\text{theo})$	\bar{M}_n LLS star (g mol ^{−1})	\bar{M}_n SEC linear (g mol ^{−1})	$f(\text{calcd})^a$
8	55 400	7 000	7.9
8	77 300	9 000	8.5
8	122 000	17 000	7.2

$$^a f = \bar{M}_n \text{ star (LLS)} / \bar{M}_n \text{ linear (SEC)}.$$

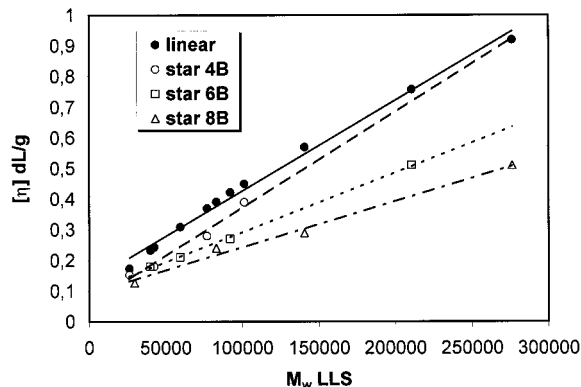


Figure 15. Evolution of the intrinsic viscosity with the molar masses for linear, tetra-, hexa-, and octaarmed PS.

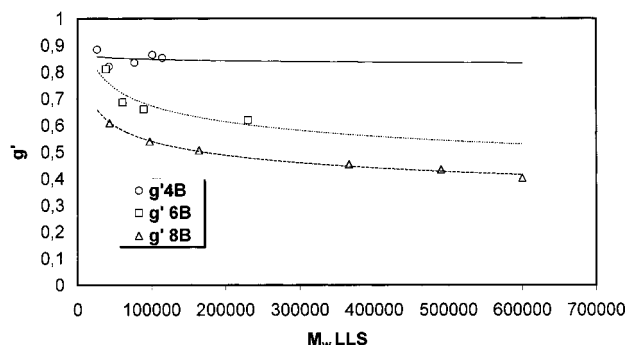


Figure 16. Evolution of g' with the molar masses for tetra-, hexa- and octaarmed PS.

As for the polydispersity of the hydrolyzed arms, it is not larger than 1.3–1.4, confirming that the tertiary alkyl bromoester functions of the octafunctional compound **6** are slow initiators of the ATRP of MMA.

5. Solution Behavior of PS, PMMA, and Pt–BuA Stars. A very accurate means to characterize stars and determine their actual functionality is to compare their intrinsic viscosity with that of linear homologues of same molar mass. To this end, the intrinsic viscosity of the tetra-, hexa-, and octafunctional PS stars prepared by our methodology were determined in toluene at 35 °C, and the values obtained were compared with those of linear PS chains, the latter obeying the following relation:³⁹ $[\eta] = 0.123 \times 10^{-3} \bar{M}_w^{0.71}$.

The data obtained are shown in Figure 15. As expected, the higher the functionality of the polymer, the lower their intrinsic viscosities for a same molar mass. Since $[\eta]$ can be directly related to the radius of gyration $\langle S^2 \rangle$ through the Fox–Flory equation

$$[\eta] = \frac{6^{3/2} \Phi \langle S^2 \rangle^{3/2}}{\bar{M}_w}$$

and considering that stars of higher functionality exhibit smaller radii of gyration, the trend observed is fully

Table 10. Comparison of the Theoretical Values of g' Calculated Using the Random Walk and the Semiempirical Models with Experimental Values of g'

F	g' RW	g' Richter	\overline{M}_w g' ^a (g mol ⁻¹)
4	0.83	0.80	0.85 (114 000) ^b
6	0.71	0.58	0.60 (484 000)
8	0.63	0.46	0.40 (790 000)

^a Results of this paper. ^b Molar masses where g' is constant.

consistent. In Table 10 are also given the experimental g' values corresponding to the ratio $[\eta]_{\text{star}}/[\eta]_{\text{linear}}$ in a good solvent (toluene at 35 °C). The g' values are also known to depend on the number of arms of star polymers; therefore, their determination is an alternative method to check the functionality of our stars. The variation of the g' values with \overline{M}_w is plotted in Figure 16.

It can be observed, on one hand, that g' decreases as the functionality of the stars increases. On the other hand, g' for stars of same functionality is found to decrease with increasing \overline{M}_w until a plateau value that is reached for star samples of relatively high molar mass ($\overline{M}_w > 10^5$ g mol⁻¹). Roovers also observed this same behavior on his multiarmed polybutadiene stars.⁴⁰

This decrease of g' with \overline{M}_w merely reflects the fact that, near the star core, the arms are forced to stretch because of the existing steric crowding. As the importance of this phenomenon vanishes with the arm size, g' then tends to decrease. This can account for the fact that octafunctional species require samples of higher molar mass than stars of lower functionality before the plateau value of g' could be reached.

These experimental results were then compared with the prediction of two theoretical models. As expected, the random walk model (RW) that is suitable for stars of a functionality lower than 6 agrees well with the behavior observed for our four functional stars. For stars of higher functionality, it is the semiempirical model of Grest et al.^{1a} that turns to be the most pertinent in our experimental context. The semiempirical relation $g' = K' f^\beta$, where K' and β values are equal to 2.37 and -0.789, respectively, leads to values that fall in excellent agreement with experimental g' determined on the hexa- and octafunctional samples.

As for the intrinsic viscosities of the octaarmed poly(*t*-BuA) stars determined in acetone and that of poly(MMA) stars obtained in toluene, they were also found lower than those of corresponding linear polymers of same molar mass, thus confirming the branched character of the materials generated from the calixarene core (Table 11).

Conclusions

This paper discusses the synthesis of star-shaped PS, poly(*tert*-butyl acrylate)s, and poly(methyl methacrylate)s by ATRP using calixarene-based multifunctional initiators. Depending upon the monomer considered, the conditions applied to obtain stars of precisely defined functionality were quite different. For instance, in the case of polystyrene stars the polymerization had to be discontinued at rather low monomer conversion to prevent stars from irreversible coupling. However, this phenomenon of star–star coupling could be alleviated to some extent upon using large $[M]_0/[initiator]_0$ ratios. Stars with \overline{M}_n as high as 6×10^5 g mol⁻¹ could

Table 11. Comparison of the Experimentally Determined Intrinsic Viscosities of PMMA and Pt–BuA Stars with the Calculated Values for the Corresponding Linear Polymers

polymer	\overline{M}_w LLS (g mol ⁻¹)	$[\eta]$ (dL g ⁻¹) linear polymer ^a	$[\eta]$ (dL g ⁻¹) star 8 arms
PMMA	83 400	0.278	0.142
	121 700	0.36	0.17
	154 200	0.435	0.19
Pt–BuA	55 000	0.168	0.066
	95 300	0.255	0.137

^a Theoretical value given by the *Polymer Handbook* for the linear PMMA in toluene at 35 °C: $[\eta]$ (dL g⁻¹) = $0.071 \times 10^{-3} M^{0.73}$ and for linear Pt–BuA in acetone at 25 °C: $[\eta]$ (dL g⁻¹) = $0.047 \times 10^{-3} M^{0.75}$.

be prepared in this way. The second part of this study was dedicated to the thorough characterization of the star samples obtained. Independent of the method used for this characterization, these ATRP-derived stars were found to exhibit the expected functionality of 4, 6, and 8.

Experimental Section

a. Materials. All materials were purchased from Aldrich. The monomers (styrene, *tert*-butyl acrylate, and methyl methacrylate) were stirred over CaH₂ and distilled under vacuum just before use. CuCl (99%), CuBr (98%), 2,2'-bipyridyl (bipy), diphenyl ether (DPE), ethylene carbonate (EC), triethylamine, potassium carbonate, 2-bromopropionyl bromide, 2-bromoisobutyl bromide, 4-*tert*-butylphenol, 4-*tert*-butylcalix[4]arene, 4-*tert*-butylcalix[6]arene, and 4-*tert*-butylcalix[8]arene were used as received. THF and acetone were stirred over CaH₂ overnight and distilled prior to use.

Synthesis of Monofunctional Initiator 4-*tert*-Butylphenyl(2-bromopropionate) (1). In a 250 mL three-neck flask equipped with a magnetic stirrer, 10 g (6.6×10^{-2} mol) of 4-*tert*-butylphenol was suspended in 80 mL of dry THF and 11.2 mL of triethylamine (7.9×10^{-2} mol). The mixture was cooled to 0 °C, and 8.4 mL (7.9×10^{-2} mol) of 2-bromopropionyl bromide dissolved in 20 mL of THF was added dropwise over a period of 1 h. The reaction mixture was stirred at room temperature overnight. The salt was removed by filtration and the crude ester obtained after concentrating the solution was dissolved in diethyl ether. The organic layer was washed successively with dilute K₂CO₃ solution and water and dried over anhydrous magnesium sulfate. The crude product was distilled under vacuum (90 °C/2 mmHg) as a colorless liquid in 80% yield. ¹H NMR (CDCl₃) δ_{ppm} : 7.47 (d, 2H, aromatic protons, a,a'; J = 8.47 Hz), 7.10 (d, 2H, aromatic protons, b,b'; J = 8.38 Hz), 4.60 (q, 1H, -CH-, J = 6.8 Hz), 1.96 (d, 3H, CH₃-, J = 6.9 Hz), 1.35 (s, 9H, *tert*-butyl). ¹³C NMR (CDCl₃) δ_{ppm} : 22.5 (CH₃-CH-Br); 32.1 (-CH₃ of *tert*-butyl), 36 (C(CH₃)₃), 40.1 (CH₃-CH-Br) 121, 127.5, 149, and 150 (aromatic carbons) and 169.8 (carbonyl). IR: $\nu(\text{COO})$ = 1680 cm⁻¹, $\nu(\text{C-Br})$ = 795 cm⁻¹.

Synthesis of Monofunctional Initiator 4-*tert*-Butylphenyl(2-bromoisobutyrate) (5). It was prepared in the same manner as that described above. 2-Bromoisobutryl bromide was used in place of 2-bromopropionyl bromide. The crude product obtained crystallized immediately after evaporation of the solvent to yield 95% of a white powder. ¹H NMR (CDCl₃) δ_{ppm} : 7.47 (d, 2H, aromatic protons, a,a'; J = 8.40 Hz), 7.10 (d, 2H, aromatic protons, b,b'; J = 8.35 Hz), 1.96 (s, 6H, CH₃), 1.35 (s, 9H, *tert*-butyl). ¹³C NMR (CDCl₃) δ_{ppm} : 31.2 ((CH₃)₂-C-Br); 32 (-CH₃ of *tert*-butyl), 35.3 (C(CH₃)₃), 56.1 (C-Br) 120.9, 126.9, 149.6, and 150 (aromatic carbons) and 171 (carbonyl). IR: $\nu(\text{COO})$ = 1680 cm⁻¹, $\nu(\text{C-Br})$ = 805 cm⁻¹.

Synthesis of Tetrafunctional Initiator 5,11,17,23-Tetra-*tert*-butyl-25,26,27,28-tetrakis(2-bromopropionyloxy) calix[4]arene (2). In a 250 mL three-neck flask equipped with a magnetic stirrer and a reflux condenser, 4 g (6.15×10^{-3} mol) of 4-*tert*-butylcalix[4]arene was suspended

in 100 mL of dry acetone. Then 5.1 g (3.7×10^{-2} mol) of potassium carbonate was added to the suspension. The mixture was warmed under reflux for 2 h. After this time, a solution of 7.8 mL (7.4×10^{-2} mol) of 2-bromopropionyl bromide in 50 mL of acetone was added dropwise. The reaction mixture was kept under reflux for 72 h. The solid materials were filtrated of salts, the filtrate isolated being concentrated and reprecipitated two times using a mixture of methanol/water (85/15 v/v). A white powder was obtained in 25% yield. ^1H NMR (CDCl_3) δ_{ppm} : 7.1 to 6.8 (m, 2H, aromatic protons), 5.4 to 4.7 (m, 1H, $-\text{CH}-$), 4 to 3.4 (m, 2H, $-\text{CH}_2-$), 2.1, 1.4 to 1 (m, 12H, CH_3- and *tert*-butyl). ^{13}C NMR (CDCl_3) δ_{ppm} : 21.8 ($\text{CH}_3-\text{CH}-\text{Br}$), 31.5 ($\text{Ar}-\text{CH}_2-\text{Ar}$), 32.2 ($-\text{CH}_3$ of *tert*-butyl), 33.8 ($\text{C}(\text{CH}_3)_3$), 39.8 ($\text{CH}_3-\text{CH}-\text{Br}$) 127.5, 131.1, 142.5, and 148.9 (aromatic carbons) and 168.1 (carbonyl). Anal. Calcd $\text{C}_{56}\text{H}_{68}\text{O}_8\text{Br}_4$: C, 56.35; H, 5.72, O, 10.77; Br, 26.94. Found: C, 57.02; H, 6.15; O, 10.34, Br, 26.50. Mass spectrum (FAB): ($\text{M}-\text{C}_3\text{H}_4\text{OBr} = 1052 \text{ g mol}^{-1}$).

Synthesis of Hexafunctional Initiator 5,11,17,23,29,35-Hexa-*tert*-butyl-37,38,39,40,41,42-hexakis(2-bromopropionyloxy)calix[6]arene (3). In a 250 mL three-neck flask, equipped with a magnetic stirrer, 3 g (1.7×10^{-3} mol) of 4-*tert*-butylcalix[6]arene was suspended in 30 mL of dry THF. A 4.3 mL aliquot of triethylamine (3×10^{-2} mol) was added, the mixture becoming homogeneous upon stirring. The solution was cooled to 0 °C, and 3.1 mL (3×10^{-2} mol) of 2-bromopropionyl bromide dissolved in 30 mL of THF was added dropwise over a period of 1 h, and then the reaction mixture was stirred at room temperature for 48 h. The solution was concentrated and precipitated using cold water. The crude solid obtained was dissolved in diethyl ether and washed successively with dilute K_2CO_3 solution and water and dried over anhydrous MgSO_4 . Ether was removed and the concentrate was reprecipitated two times using a mixture of methanol/water (90/10 v/v). A white powder was obtained in 76% yield. ^1H NMR (CDCl_3) δ_{ppm} : 7.5 to 6.7 (s, 2H, aromatic protons), 4.7 and 2.8 (s, 1H, $-\text{CH}-$), 4 to 3.2 (s, 2H, $-\text{CH}_2-$), 2.3 and 1.6 to 0.9 (m, 12H, CH_3- and *tert*-butyl). ^{13}C NMR (CDCl_3) δ_{ppm} : 21.6 ($\text{CH}_3-\text{CH}-\text{Br}$), 31 ($\text{Ar}-\text{CH}_2-\text{Ar}$), 31.4 ($-\text{CH}_3$ of *tert*-butyl), 34.4 ($\text{C}(\text{CH}_3)_3$), 38.7 ($\text{CH}_3-\text{CH}-\text{Br}$) 125, 130.8, 143, and 148.9 (aromatic carbons) and 169 (carbonyl). Anal. Calcd $\text{C}_{84}\text{H}_{102}\text{O}_{12}\text{Br}_6$: C, 56.35; H, 5.72, O, 10.77; Br, 26.94. Found: C, 56.64; H, 5.41; O, 10.80; Br, 27.15. Mass spectrum (FAB): $M_w(\text{C}_3\text{H}_4\text{OBr}) = 1647 \text{ g mol}^{-1}$; $M_w(2(\text{C}_3\text{H}_4\text{OBr})) = 1511 \text{ g mol}^{-1}$.

Synthesis of Octafunctional Initiator 5,11,17,23,29,35,41,47-Octa-*tert*-butyl-49,50,51,52,53,54,55,56-octakis(2-bromopropionyloxy)calix[8]arene (4). It was prepared in the same manner as that described above to yield 76% of a white powder. ^1H NMR (CDCl_3) δ_{ppm} : 7.1 (s, 2H, aromatic protons), 4.4 (s, 1H, $-\text{CH}-$), 3.7 (s, 2H, $-\text{CH}_2-$), 1.6 (s, 3H, CH_3-), 1.2 (s, 9H, *tert*-butyl). ^{13}C NMR (CDCl_3) δ_{ppm} : 21.4 ($\text{CH}_3-\text{CH}-\text{Br}$), 30.5 ($\text{Ar}-\text{CH}_2-\text{Ar}$), 31.2 ($-\text{CH}_3$ of *tert*-butyl), 34.3 ($\text{C}(\text{CH}_3)_3$), 39.1 ($\text{CH}_3-\text{CH}-\text{Br}$) 126.1, 130.8, 144.5, and 148.9 (aromatic carbons) and 167.8 (carbonyl). Anal. Calcd $\text{C}_{112}\text{H}_{136}\text{O}_{16}\text{Br}_8$: C, 56.35; H, 5.72, O, 10.77; Br, 26.94. Found: C, 55.72; H, 5.43; O, 10.76; Br, 27.75. Mass spectrum (FAB): $M_w(\text{C}_3\text{H}_4\text{OBr}) = 2241 \text{ g mol}^{-1}$; $M_w(2(\text{C}_3\text{H}_4\text{OBr})) = 2105 \text{ g mol}^{-1}$.

Synthesis of Octafunctional Initiator 5,11,17,23,29,35,41,47-Octa-*tert*-butyl-49,50,51,52,53,54,55,56-octakis(2-bromoisobutyryloxy)calix[8]arene (6). It was prepared in the same manner as that described above. 2-Bromoisobutyryl bromide was used in place of 2-bromopropionyl bromide. The concentrate was reprecipitated two times using a pure methanol, a white powder being obtained in 78% yield. ^1H NMR (CDCl_3) δ_{ppm} : 7.2 (s, 2H, aromatic protons), 3.7 (s, 2H, $-\text{CH}_2-$), 2.1 (s, 3H, CH_3-), 1.2 (s, 9H, *tert*-butyl). ^{13}C NMR (CDCl_3) δ_{ppm} : 29.9 ($\text{Ar}-\text{CH}_2-\text{Ar}$), 30.5 ($\text{CH}_3-\text{C}-\text{Br}$), 31.2 ($-\text{CH}_3$ of *tert*-butyl), 34.3 ($\text{C}(\text{CH}_3)_3$), 54.7 ($\text{CH}_3-\text{C}-\text{Br}$), 129, 130.8, 146, and 148.8 (aromatic carbons) and 170 (carbonyl). Anal. Calcd $\text{C}_{120}\text{H}_{152}\text{O}_{16}\text{Br}_8$: C, 57.9; H, 6.1, O, 10.3; Br, 25.7. Found: C, 56.7; H, 6.36; O, 10.19; Br, 24.88. Mass spectrum (FAB): $M_w(\text{C}_4\text{H}_6\text{OBr}) = 2339 \text{ g mol}^{-1}$.

b. Polymerization Procedures. ATRP of Styrene. A typical example is given below. The polymerization was carried out in a Schlenk flask. It was charged with the monofunctional

1 (150 mg, 5.26×10^{-4} mol), CuBr (75.5 mg, 5.26×10^{-4} mol), 2,2'-bipyridyl (246 mg, 1.57×10^{-3} mol) and 6.5 mL of styrene. The reaction solution was submitted to three freeze–vacuum–thaw cycles to remove evacuated gases. The flask was then placed in an oil bath thermostated at 100 °C. After vigorous stirring the flask was cooled at room temperature, and the contents were dissolved in THF and then passed through a column of neutral alumina to remove copper salts. The polymer was precipitated using an excess of ethanol, filtered, and dried at 50 °C under vacuum for 24 h. The conversion was obtained gravimetrically.

ATRP of Methyl Methacrylate. A Schlenk was charged with the monofunctional initiator **5** (70 mg, 2.34×10^{-4} mol), CuCl (23.2 mg, 2.34×10^{-4} mol), 2,2'-bipyridyl (73 mg, 4.68×10^{-4} mol), diphenyl ether (7.5 mL, 50% v/v), and MMA (7.5 mL). Following the same procedure described as that previously described, the solution was placed in an oil bath at 90 °C. The polymer obtained was then precipitated using methanol after filtrating copper salts.

ATRP of *tert*-Butyl Acrylate. A Schlenk was charged with the monofunctional initiator **1** (100 mg, 7×10^{-4} mol), CuBr (100 mg, 7×10^{-4} mol), 2,2'-bipyridyl (219 mg, 1.4×10^{-3} mol), ethylene carbonate (1 g, 10% v/v), and *tert*-butyl acrylate (10 mL). Following the same procedure as that described above, the solution was placed in an oil bath at 100 °C. The polymer obtained was then precipitated using a mixture of methanol/water (90/10 v/v) after filtrating copper salts.

Hydrolysis of the Star Polymer. A 0.3 g sample of a multifunctional star polymer was dissolved in 20 mL of THF in a 250 mL round-bottomed flask fitted with a condenser and N_2 inlet. A 2 mL aliquot of KOH (1 M solution in ethanol) was then added, and the solution was refluxed for 10 min. The solution was evaporated to dryness, dissolved in THF, and precipitated using methanol and finally dried.

Characterization. NMR spectra were obtained using a Bruker AC200 NMR spectrometer. CDCl_3 was used as a solvent. Apparent molar masses of polystyrene stars were determined using size exclusion chromatography apparatus equipped with a Varian refractive index detector and a JASCO 875 UV/vis absorption detector, the SEC line itself being constituted of three TSK columns (10^4 , 1500, and 250 Å). Calibration was performed using linear polystyrene standards. The actual molar masses of the stars polymers were calculated from the response of a multiangle laser light scattering detector (Wyatt Technology) that was purposely connected to the size exclusion chromatography (MALLS/SEC) line. The dn/dc values for the star polymers were measured in THF, at 25 °C, with a laser source operating at 633 nm and were found to be the same as that of the linear polymer ($\text{dn}/\text{dc} = 0.183$ for PS, 0.087 for PMMA, and $0.060 \text{ cm}^3 \text{ g}^{-1}$ for Pt–BuA).

References and Notes

- (1) (a) Grest, G. S.; Fetters, L. J.; Huang, J. S.; Richter, D. *Advances in Chemical Physics*; Prigogine, I., Rice, S. A., Eds.; John Wiley & Sons: New York, 1996; Vol. XCIV. (b) Hadjichristidis, N.; Pispas, S.; Pitsikalis, M.; Iatrou, H.; Vlahos, C. *Adv. Polym. Sci.* **1998**, *142*, 71. (c) Burchard, W. *Adv. Polym. Sci.* **1998**, *143*.
- (2) (a) Matyjaszewski, K. *J. Phys. Org. Chem.* **1995**, *8*, 197. (b) Webster, O. W. *Science* **1991**, *251*, 887. (c) Quirk, R. P. In *Polymer Science and Technology*; Plenum Press: New York, 1985; Vol. 31, p 321.
- (3) (a) David, B. A.; Kinning, D. J.; Thomas, E. L.; Fetters, L. J. *Macromolecules* **1986**, *19*, 215. (b) Hadjichristidis, N.; Guyot, A. N.; Fetters, L. J. *Macromolecules* **1978**, *11*, 668. (c) Morton, M.; Helminiak, T. E.; Gadkary, S. D.; Bueche, F. *J. Polym. Sci.* **1962**, *57*, 471. (d) Iatrou, H.; Hadjichristidis, N. *Macromolecules* **1992**, *25*, 4649. (e) Iatrou, H.; Hadjichristidis, N. *Macromolecules* **1993**, *26*, 2479. (f) Mays, J. W. *Polym. Bull.* **1990**, *23*, 247. (g) Schulz, G. O.; Milkovich, R. *J. Appl. Polym. Sci.* **1982**, *27*, 4773. (h) Roovers, J.; Zhou, L.; Toporowski, P. M.; Van Der Zwan, M.; Iatrou, H.; Hadjichristidis, N. *Macromolecules* **1993**, *26*, 4324.
- (4) (a) Cloutet, E.; Fillaut, J. L.; Astruc, D.; Gnanou, Y. *Macromolecules* **1998**, *31*, 6748. (b) Jacob, S.; Majoros, I.; Kennedy, J. P. *Macromolecules* **1996**, *29*, 8631. (c) Shohi, H.; Sawamoto,

- M.; Higashimura, T. *Makromol. Chem.* **1992**, *193*, 2027. (d) Schappacher, M.; Deffieux, A. *Macromolecules* **1992**, *25*, 6744. (e) Chang, J. Y.; Ji, H. J.; Han, M. J.; Cheong, S. B.; Yoon, M. *Macromolecules* **1994**, *27*, 1376. (f) Cloutet, E.; Fillaut, J.-L.; Astruc, D.; Gnanou, Y. *Macromolecules* **1999**, *32*, 1043.
- (5) Fukui, H.; Deguchi, T.; Sawamoto, M.; Higashimura, T. *Macromolecules* **1996**, *29*, 1131.
- (6) (a) Quirk, R.; Tsai, Y. *Macromolecules* **1998**, *31*, 8016. (b) Fijumoto, T.; Tani, S.; Takano, K.; Ogawa, M.; Nagasawa, M. *Macromolecules* **1978**, *11*, 673. (c) Gnanou, Y.; Lutz, P.; Rempp, P. *Makromol. Chem.* **1988**, *189*, 2885. (d) Comanita, B.; Noren, B.; Roovers, J. *Macromolecules* **1999**, *32*, 1069. (e) Six, J.-L.; Gnanou, Y. *Macromol. Symp.* **1995**, *95*, 137.
- (7) Moad, G.; Solomon, D. H. *The Chemistry of Free-Radical Polymerization*; Pergamon: Oxford, 1995.
- (8) (a) Georges, M. K.; Veregin, R. P. N.; Kazmaier, P. M.; Hamer, G. K. *Trends Polym. Sci.* **1994**, *2*, 66. (b) Davis, T. P.; Kukulj, D.; Haddleton, D. M.; Maloney, D. R. *Trends Polym. Sci.* **1995**, *3*, 365. (c) Hawker, C. J. *Trends Polym. Sci.* **1996**, *4*, 183. (d) Sawamoto, M.; Kamigaito, M. *Trends Polym. Sci.* **1996**, *4*, 371. (e) Colombani, D. *Prog. Polym. Sci.* **1997**, *22*, 1649. (f) Hawker, C. J. *Acc. Chem. Res.* **1997**, *30*, 373. (g) Sawamoto, M.; Kamigaito, M. *Polymer Synthesis (Materials Science and Technology Series)*; Schlüter, A.-D., Ed.; VCH-Wiley: Weinheim, Germany; Chapter 6, in press. (h) Matyjaszewski, K. *Controlled Radical Polymerization*; ACS Symposium Series 685; American Chemical Society: Washington, DC, 1998.
- (9) (a) Patten, T. E.; Xia, J.; Abernathy, T.; Matyjaszewski, K. *Science* **1996**, *9*, 8576. (b) Granel, C.; Dubois, Ph.; Jérôme, R.; Teyssié, Ph. *Macromolecules* **1996**, *9*, 8576. (c) Percec, V.; Barboiu, B. *Macromolecules* **1996**, *29*, 3665. (e) Kotani, Y.; Kato, M.; Kamigaito, M.; Sawamoto, M. *Macromolecules* **1996**, *29*, 6979.
- (10) (a) Chiefari, J.; Chong, Y. K.; Ercole, F.; Krstina, J.; Jeffery, J.; Le, T. P.; Mayadunne, R. T.; Meijs, G. F.; Moad, C. L.; Moad, G.; Rizzardo, E.; Thang, S. H. *Macromolecules* **1998**, *31*, 5559. (b) Chong, Y. K.; Le, T. P.; Moad, G.; Rizzardo, E.; Thang, S. H. *Macromolecules* **1999**, *32*, 2071.
- (11) Wayland, B. B.; Poszmik, G.; Mukerjee, S. L.; Fryd, M. J. *Am. Chem. Soc.* **1994**, *116*, 7943.
- (12) (a) Wang, J. S.; Matyjaszewski, K. *J. Am. Chem. Soc.* **1995**, *117*, 5614. (b) Matyjaszewski, K.; Patten, T. E.; Xia, J. *J. Am. Chem. Soc.* **1997**, *119*, 674.
- (13) (a) Shipp, D. A.; Wang, J.-L.; Matyjaszewski, K. *Macromolecules* **1998**, *31*, 8005. (b) Jo, S. M.; Gaynor, S. G.; Matyjaszewski, K. *Am. Chem. Soc., Polym. Prepr.* **1996**, *37* (2), 272. (c) Chen, X.; Ivan, B.; Kops, J.; Batsberg, W. *Polym. Bull.* **1997**, *39*, 559.
- (14) Matyjaszewski, K.; Beers, K. L.; Kern, A.; Gaynor, S. G. *J. Polym. Sci., Part A: Polym. Chem.* **1998**, *36*, 823. (b) Paik, H.-J.; Gaynor, S. G.; Matyjaszewski, K. *Macromol. Rapid Commun.* **1998**, *19*, 47. (c) Beers, K. L.; Gaynor, S. G.; Matyjaszewski, K.; Sheiko, S. S.; Möller, M. *Macromolecules* **1998**, *31*, 9413.
- (15) (a) Matyjaszewski, K.; Gaynor, S. G.; Kulfan, A.; Podwika, M. *Macromolecules* **1997**, *30*, 5192. (b) Gaynor, S. G.; Edelman, S.; Matyjaszewski, K. *Macromolecules* **1996**, *29*, 1079.
- (16) Hawker, C. J. *Angew. Chem., Int. Ed. Engl.* **1995**, *34*, 1456.
- (17) (a) Wang, J. S.; Greszta, D.; Matyjaszewski, K. *Polym. Mater. Sci. Eng.* **1995**, *73*, 416. (b) Matyjaszewski, K.; Miller, P. J.; Fossum, E.; Nakagawa, Y. *Appl. Organomet. Chem.* **1998**, *12*, 667. (c) Matyjaszewski, K.; Miller, P. J.; Pyun, J.; Kickelbick, G.; Diamanti, S. *Macromolecules* **1999**, *32*, 6526. (d) Zhang, X.; Xia, J.; Matyjaszewski, K. *Macromolecules* **2000**, *33*, 2340.
- (18) (a) Ueda, J.; Matsuyama, M.; Kamigaito, M.; Sawamoto, M. *Macromolecules* **1998**, *31*, 55. (b) Ueda, J.; Kamigaito, M.; Sawamoto, M. *Macromolecules* **1998**, *31*, 6762.
- (19) Kasko, A. M.; Heintz, A. M.; Pugh, C. *Macromolecules* **1998**, *31*, 256.
- (20) Angot, S.; Murthy, K. S.; Taton, D.; Gnanou, Y. *Macromolecules* **1998**, *31*, 7218.
- (21) (a) Hedrick, J. L.; Tröllsas, M.; Hawker, C. J.; Atthoff, B.; Claesson, H.; Heise, A.; Miller, R. D.; Mecerreyes, D.; Jérôme, R.; Dubois, Ph. *Macromolecules* **1998**, *31*, 8691. (b) Heise, A.; Hedrick, J. L.; Tröllsas, M.; Miller, R. D.; Franck, C. W. *Macromolecules* **1999**, *32*, 231. (c) Heise, A.; Hedrick, J. L.; Franck, C.; Miller, R. D. *J. Am. Chem. Soc.* **1999**, *121*, 8647.
- (22) Collins, J. E.; Fraser, K. L. *Macromolecules* **1998**, *31*, 6715.
- (23) (a) Percec, V.; Barboiu, B.; De, B. B.; Kim, H. G.; Smith, J. D.; Van der Sluis, M.; Grubbs, B. H.; Fréchet, J. M. J. *Am. Chem. Soc., Polym. Prepr., PMSE* **1999**, *20*, 457. (b) Kraus, A.; Robello, R. *Am. Chem. Soc., Polym. Prepr.* **1999**, *40* (2), 413.
- (24) (a) Haddleton, D. M.; Edmonds, R.; Heming, A. M.; Kelly, E. J.; Kukulj, D. *New J. Chem.* **1999**, *23*, 477. (b) Hovestad, N.; Jastrzebski, J. T. B. H.; Van Koten, G.; Bon, S. A.; Waterson, C.; Haddleton, D. M. *Am. Chem. Soc., Polym. Prepr.* **1999**, *40* (2), 393. (c) Haddleton, D. M.; Waterson, C. *Macromolecules* **1999**, *32*, 8732.
- (25) Muehlebach, A.; Rime, F.; Pfeiffer, U. *Am. Chem. Soc., Polym. Prepr.* **1999**, *40* (2), 332.
- (26) Matyjaszewski, K. *J. Macromol. Sci., Pure Appl. Chem.* **1997**, *A34* (10), 1785.
- (27) (a) Davis, K.; Charleux, B.; Matyjaszewski, K. *J. Polym. Sci., Part A: Polym. Chem.* **2000**, *38*, 2274. (b) Davis, K.; Matyjaszewski, K. *Macromolecules* **2000**, *33*, 4039.
- (28) Matyjaszewski, K.; Wang, J.-L.; Grimaud, T.; Shipp, D. A. *Macromolecules* **1998**, *31*, 1527.
- (29) Vicens, J.; Bohmer, V. *Calixarenes, a versatile class of macrocyclic compounds*; Kluwer Academic Publishers: Dordrecht, 1991.
- (30) (a) Gutsche, C. D. *Acc. Chem. Res.* **1983**, *16*, 161. (b) Bohmer, V. *Angew. Chem., Int. Ed. Engl.* **1995**, *34*, 713. (c) Ikeda, A.; Shinkai, S. *Chem. Rev.* **1997**, *97*, 1713. (d) Gutsche, C. D.; Bauer, L. J. *J. Am. Chem. Soc.* **1985**, *107*, 6059. (e) Neri, P.; Grazia, M.; Consoli, L.; Cunsolo, F.; Geraci, C.; Piatelli, M. *New J. Chem.* **1996**, *20*, 433.
- (31) Gravett, D. M.; Guillet, J. E. *Macromolecules* **1996**, *29*, 617.
- (32) Shipp, D. A.; Matyjaszewski, K. *Macromolecules* **1999**, *32*, 2948.
- (33) Fayt, R.; Forte, R.; Jacob, C.; Jérôme, R.; Ouhadi, T.; Teyssié, Ph.; Varshney, S. K. *Macromolecules* **1987**, *20*, 1442.
- (34) Matyjaszewski, K.; Nakagawa, Y.; Jasieczek, C. B. *Macromolecules* **1998**, *31*, 1535.
- (35) Moineau, G.; Minet, M.; Dubois, Ph.; Teyssié, Ph.; Senninger, T.; Jérôme, R. *Macromolecules* **1999**, *32*, 27.
- (36) Moineau, G.; Granel, C.; Dubois, Ph.; Jérôme, R.; Teyssié, Ph. *Macromolecules* **1998**, *31*, 542.
- (37) Percec, V.; Barboiu, B.; Kim, H.-J. *J. Am. Chem. Soc.* **1998**, *120*, 305.
- (38) *Polymer Handbook*, 4th ed.; Wiley-Interscience: New York, pVII/1.
- (39) Roovers, J.; Toporowski, P.; Martin, J. *Macromolecules* **1989**, *22*, 1897.

MA000570J